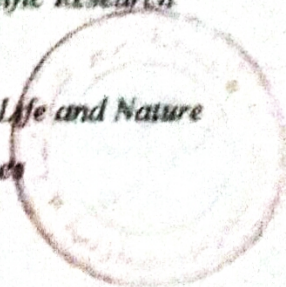


Democratic And Popular Republic of Algeria  
Ministry of Higher Education and Scientific Research  
Larbi Tebessi University  
Faculty of Exact Sciences and Sciences of Life and Nature  
Department of Matter Sciences



**MASTER'S THESIS**

**Field: Matter Sciences**

**Discipline: Physics**

**Option: Condensed Matter Physics**

**Theme:**

**Shell model study of the astro-  
physical rp reaction  $^{25}\text{Al}(p,\gamma)^{26}\text{Si}$**

**Presented by:**

*LAIDOUDI Hanadi*

**Board of Examiners**

<b><u>Chair:</u></b>	ZIAR Toufik	MCA	Tebessa Larbi Tebessi University
<b><u>Supervisor:</u></b>	BOUHELAL Mouna	professor	Tebessa Larbi Tebessi University
<b><u>Examiner:</u></b>	SERDOUK Fadhila	MCB	Tebessa Larbi Tebessi University

**Date of defence: 25/06/2019**



*Democratic And Popular Republic of Algeria*  
*Ministry of Higher Education and Scientific Research*  
*Larbi Tebessi University*  
*Faculty of Exact Sciences and Sciences of Life and Nature*  
*Department of Matter Sciences*



**MASTER'S THESIS**

**Field: Matter Sciences**

**Discipline: Physics**

**Option: Condensed Matter Physics**

**Theme:**

**Shell model study of the astro-  
physical rp reaction  $^{25}\text{Al}(p,\gamma)^{26}\text{Si}$**

**Presented by:**

*LAIDOUDI Hanadi*

**Board of Examiners**

**Chair:** ZIAR Toufik MCA Larbi Tebessi University

**Supervisor:** BOUHELAL Mouna Professor Larbi Tebessi University

**Examiner:** SERDOUK Fadhila MCB Larbi Tebessi University

**Date of defence: 25/06/2019**

Thesis achieved  
at  
*Laboratoire de Physique Appliquée et Théorique LPAT*



## **Acknowledgements**

---

*I thank first the Almighty ALLAH for giving me the power and the will, the chance to continue to complete this work. I strongly express my deep appreciation to Ms. BOUHELAL Mouna, Professor at the University of Tebessa, for leading this subject to permanent*



monitoring, sound advice, and the constant help she gave me during the development of this work. I thank Mr. ZIAR Toufik, Lecturer A at the University of Tebessa, for the honour he did in chairing the jury of my thesis. I express my thanks to Ms. SERDOUK Fadhila, Lecturer B at the University Tebessa, who agreed

*to be examiner of this thesis. I address  
my warm thanks to all my friends from  
anywhere and also for their presence  
and assistance.*

## *Dedication*

---

I am dedicating this thesis TO beloved people who have meant and continue to mean so much to me.

First and foremost, to my father Tahar LAIDOUDI and lovely mother whose love for me knew no bounds and, who taught me the value of hard work. Thank you so much “papa, mama”.

Next I also want to remember my sisters AND my brothers to my little ‘DJAD’ last but not least I am dedicating this to all my friends

To my professor Mouna bouhelal



Abstract

Résumé

ملخص

---

# Abstract

---

Nuclear shell model study focuses on the description of the energy spectra and electromagnetic properties using a compatible effective interaction with an appropriate model space. These properties are a severe test of the interaction. This model can serve many experimental studies, especially, those concentrated on astrophysics.

Our work is like a brief introduction to astrophysics, which exposes different modes of element synthesis with a simple look. We are interested to one of the most important element that has an astrophysical interest, which is Silicon. The evaluation of silicon importance shows that it is abundant in the solar system, even in the entire space.

The aim of our work is to contribute to the study of the astrophysical  $r$ - $p$  reaction:  $^{25}\text{Al}(p,\gamma)^{26}\text{Si}$ . We calculated the spectroscopic properties of  $^{26}\text{Si}$  in order to determine the spin/parity assignments of states of astrophysical interest above of the proton threshold 5513.8 keV. These levels are essential to calculate the studied reaction rate.

## Résumé

---

*L'étude de modèle en couches nucléaire se concentre sur la description des spectres en énergie et des propriétés électromagnétiques à l'aide d'une interaction effective compatible avec un espace de modèle approprié. Ces propriétés sont une rude épreuve de l'interaction. Ce modèle peut servir de nombreuses études expérimentales, en particulier, celles concentrées sur l'astrophysique.*

*Notre travail est comme une brève introduction à l'astrophysique, qui expose les différents modes de synthèse de l'élément avec une simple vue. Nous nous intéressons à l'un des éléments les plus importants qui a un intérêt astrophysique, qui est le Silicium. L'évaluation de l'importance du silicium montre qu'il est abondant dans le système solaire, même dans l'ensemble de l'espace.*

*Le but de notre travail est de contribuer à l'étude de la réaction astrophysique r-p :  $^{25}\text{Al}(p,\gamma)^{26}\text{Si}$ . Nous avons calculé les propriétés spectroscopiques du  $^{26}\text{Si}$  afin de déterminer les attributions de spin/parité des états d'intérêt astrophysique au-dessus du seuil de l'émission proton 5513.8 keV. Ces niveaux sont indispensables pour calculer le taux de la réaction étudiée.*



## ملخص

دراسة نموذج الطبقات النووي يركز على وصف أطياف الطاقة والخصائص الكهرومغناطيسية باستخدام تفاعل فعال مناسب لفضاء منطقة التكافؤ المختار. هذه الخصائص تعد اختبارا للتفاعل. هذا النموذج يمكن أن يخدم العديد من الدراسات التجريبية، وخاصة تلك التي تتركز في الفيزياء الفلكية.

هذا العمل عبارة عن مقدمة موجزة للفيزياء الفلكية التي تعرض تركيب العناصر في الفضاء بنظرة مبسطة لمختلف انماط هذا التركيب. ركزنا في عملنا هذا على عنصر يعتبر من أهم العناصر التي لها أهمية بالغة في الفيزياء الفلكية، ألا وهو السيليكون. تقييم أهمية السيليكون بينت توفره في النظام الشمسي، بل وحتى في كافة الفضاء الخارجي.

هدف عملنا هذا هو المشاركة في دراسة التفاعل الفلكي من نوع  $^{25}Al(p,\gamma)^{26}Si$ . قمنا بحساب الخصائص الطيفية ل  $^{26}Si$  وهذا لإيجاد الزوجية و السبين النووي للمستويات الطاقوية التي لها جانب و دور هام في الفيزياء الفلكية ما فوق طاقة العتبة لإصدار بروتون  $5513 \text{ keV}$ . هذه المستويات لها أهمية كبرى في حساب نسبة التفاعل المدروس.

# Table of Contents

Abstract	i	
Résumé	ii	
ملخص	iii	
Dedications	iv	
Acknowledgments	vi	
list of Tables	viii	
List of Figures	ix	
List of Symbols		x
General Introduction	1	
Chapter I: Astrophysical interest of silicon		3
<hr/>		
1. Nuclear Astrophysics		4
2. Nucleosynthesis	4	
2.1 nucleosynthesis in the big bang	5	
2.2 synthesis of elements in stars		5
3. Modes of element synthesis	6	
3.1 The rapid neutron-capture process		6
3.2 The slow neutron-capture process	7	
3.3 the proton capture process		7
4. Silicon abundance in solar system	8	
5. Silicon-burning process	9	
Chapter II: Shell model and sd shell nuclei		10
1. A brief history of nuclear models		10
1.1 Liquid-drop Model		10
1.2 Shell Model		11
1.3 Independent-particle Model	11	
2. Nuclear shell model and energy spectra		11
2.1 Magic numbers		11
2.2 Independent particle		11
3. General many-body problem for fermions	13	
4. Ingredients of the shell model	14	
5. Electromagnetic moments and transitions	15	
5.1 Electric operator	15	
5.2 Magnetic operator	16	
5.3 Reduced probabilities of electromagnetic transitions		16
6. Nuclei of the sd shell		17
7. Electromagnetic transitions in the sd nuclei	18	
8. Isospin	19	
Chapter III: Spectroscopic study of the $^{26}\text{Si}$ : levels of astrophysical interest		20
1. Study of the Si spectroscopic properties		20
I.1. Energy spectra	20	
I.2. Electromagnetic transitions	23	
2. States of astrophysical interest in $^{26}\text{Si}$		25
General conclusion		28
Bibliographies		29

# List of Tables

---

<u>Table No</u>	<u>Title</u>	<u>Page</u>
Table I.1:	<i>Evolution of a 15-solar-mass star [5], Myr means "million years".</i>	8
Table II.2	<i>Adjusted parameters for E2, M1 and E3 transitions (see text).</i>	18
Table III.1:	<i>Comparison theoretical versus experimental [3] energy spectra of the isospin triplet <math>T=1</math> states in <math>A=26</math> nuclei, <math>^{26}\text{Mg}</math>, <math>^{26}\text{Al}</math>, and <math>^{26}\text{Si}</math>.</i>	22
Table III.2	<i>Comparison experimental [3] versus calculated spectroscopic properties of the <math>^{26}\text{Si}</math>.</i>	25
Table III.3:	<i>Proposed of <math>J^\pi</math> assignments for levels in <math>^{26}\text{Si}</math> having astrophysical interest.</i>	27



# List of Figures

---

<u>Figure N°</u>	<u>Titel</u>	<u>Page</u>
Figure I-1:	<i>Abundances of the chemical elements in the Solar System.</i>	3
<i>Figure I-2</i>	<i>Chart resumes Nucleosynthesis.</i>	4
<i>Figure I-3</i>	<i>Chart shows the “Big Bang story”.</i>	5
<i>Figure I-4</i>	<i>Chart resumes Modes of Element Synthesis.</i>	6
<i>Figure I-5</i>	<i>Nuclear chart [3], on which are shown nuclei produced through the r-process mode.</i>	7
<i>Figure I-6</i>	<i>Nucleosynthesis of proton-rich nuclei via rapid proton capture.</i>	8
<i>Figure I-7</i>	<i>Type II-P supernova in the Large Magellanic Cloud. NASA image [5].</i>	9
<i>Figure II-1</i>	<i>Graphic configuration of the shell model single-particle orbitals.</i>	12
<i>Figure II-2</i>	<i>Gamma emission in a nucleus.</i>	15
<i>Figure II-3</i>	<i>The sd shell nuclei Chart [3].</i>	17
<i>Figure II-4</i>	<i>Diagram of the first orbitals forming the ground state of <math>^{26}\text{Si}</math>.</i>	18

# *List of Symbols*

---

$r$ -process	<i>rapid neutron-capture process</i>
$s$ -process	slow neutron-capture process
$p$ -process	proton capture process
AGB stars	Asymptotic Giant Branch stars
GCE	Galactic Chemical Evolution
$v_{OH}$	harmonic-oscillator potential
$H_0$	the independent movement of nucleons in the nucleus
$\omega$	the harmonic-oscillator frequency
$E_i$	initial state energy
$E_f$	final state energy
$h_i$	The Hamiltonian of an individual nucleon
$v_{ij}$	two-body interaction between the nucleons $i$ and $j$
$H_r$	the residual interaction
$\mu_r$	the nuclear magneton
$\Gamma_\gamma, \Gamma_w$	The transition widths and the Weisskopf estimate, respectively
$S$	the strength of a transition
$\tau_m$	Mean lifetime
$T_{1/2}$	Half-life
USDA	Effective interaction
USDB	Effective interaction
USD	Effective interaction
PSDPF	Effective interaction
EL	electrical transition
ML	magnetic transition
$L$	multipolarity of a radiation (photon orbital momentum)
$e_p$	the effective charge of proton
$e_n$	the effective neutron charge
$Z$	number of protons
$N$	number of neutrons
$A$	atomic number
$\pi_\gamma$	the parity of a gamma transition
$E_{th}$	theoretical energy
$E_{exp}$	experimental energy
$\Delta$	the difference in energy
$Y_{LM}$	spherical harmonics
$0\hbar\omega$ states	(0 particle-0 hole jump) denotes the positive parity states
$1\hbar\omega$ states	(1 particle-1 hole jump) denotes the negative parity states
$g^s, g^l$	Gyromagnetic factors of spin and orbit, respectively
$e(k)$	the nucleon $k$ effective charge
$Q$	electric charge
$T$	Isospin



*General*  
*Introduction*

# General Introduction

---

**A**strophysics is the branch of astronomy that uses physics disciplines to study the different astronomical objects such as planets, stars, galaxies and others, in order to explore all their properties, motions and positions.

Nuclear astrophysics is a collaboration of both astronomy and nuclear physics, which realize an improvement to understand the origin of the chemical elements and the energy generation in astronomical objects like stars.

Nucleosynthesis, nuclear reactions in massive stars, by fusion of lighter elements into heavier ones, occurs during sequential hydrostatic burning processes called hydrogen burning, helium burning, carbon burning, oxygen burning, and silicon burning. Hydrogen requires a lower temperature than helium; helium requires a lower temperature than carbon, and so.

Silicon is the seventh most abundant element in the solar system; elements synthesized are created by different modes of synthesis processes.

The astrophysical Rapid Proton Capture (r-p) process creates some silicon isotopes. As an example we quote the  $^{25}\text{Al}(p,\gamma)^{26}\text{Si}$  reaction; reaction that attracted our attention.

Shell model calculations have proved their efficiency to describe not only the energy spectra of nuclei in different mass parts, but also other nuclear properties such as electromagnetic transitions, electromagnetic moments and spectroscopic factors.

In our work we calculated the spectroscopic properties of  $^{26}\text{Si}$  in order to determine the spin/parity assignments of states of astrophysical interest above of the proton threshold, 5513.8 keV. These levels are essential to calculate the reaction rate.

This manuscript contains three fundamental chapters distributed as the following:

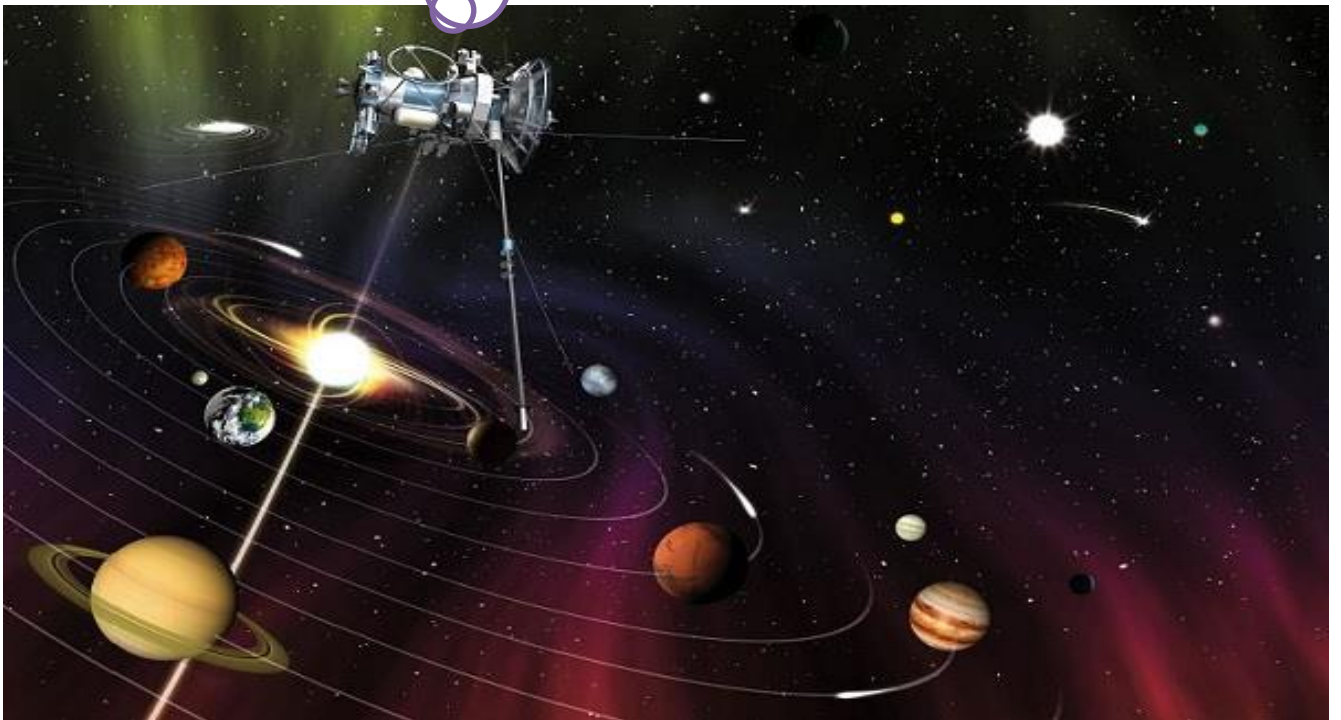
✓ **Chapter I** presents an introduction to astrophysics focusing on reactions and their different processes.

✓ *Chapter II* reminds the basics of the nuclear shell model and electromagnetic transition properties. A brief outline of the properties of the sd shell nuclei will be given.

✓ *Chapter III* is dedicated to the discussion of the obtained spectroscopic properties results and their comparison to experimental available data, especially, those concerning states of astronomical interest for  $^{26}\text{Si}$ . Important prediction will be proposed.

This dissertation ends with a general conclusion.

# Chapter I



# Chapter I

## *Astrophysical Interest of Silicon*

---

Our universe is supposed to have formed about 15 billion years ago in a hot dense fireball, the big bang. As time progressed, the universe expanded and cooled. After a microsecond, a soup of quarks and gluons condensed into protons and neutrons and the era of nuclear physics began. After another 10 seconds, the universe had cooled to the point that the lightest nuclei, isotopes of hydrogen, helium and a tiny amount of lithium, could form. These nuclei are the ashes of the earliest element forming processes that begins with nuclear reactions among nuclei of these three elements [1]. As an example, we show on Figure I-1 the chemical elements abundant in the solar system.

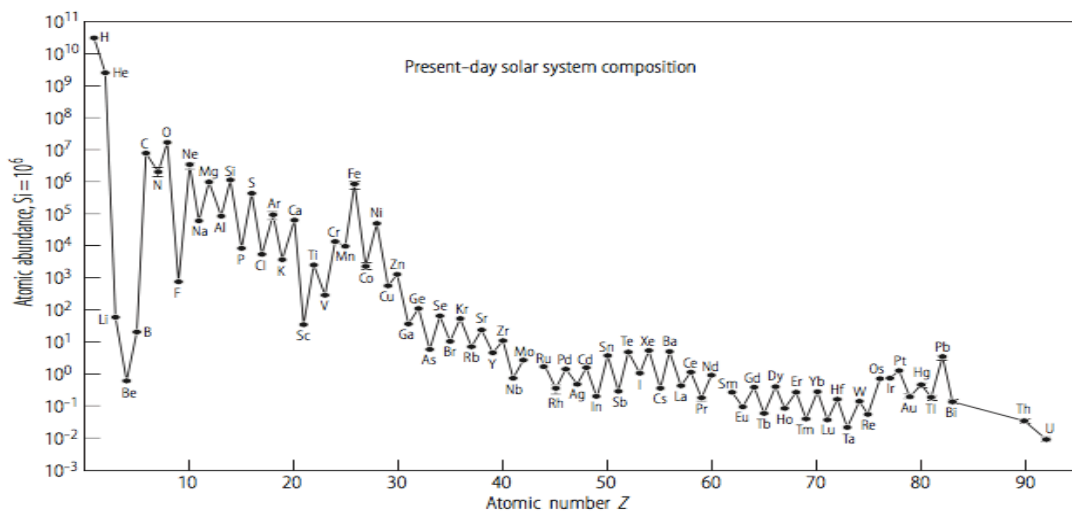


**Figure I-1:** *Abundances of the chemical elements in the solar system [2].*

In this chapter we will present a short introduction to astrophysical reactions occur in the stellar core and their different processes with an overview to the rp reaction of our interest.

### **1. *Nuclear Astrophysics***

Nuclear astrophysics is that branch of astrophysics, which helps understanding the universe, or at least some of its many faces, through the knowledge of the atomic nucleus.



Nuclear structure and nuclear astrophysics are intricately connected. Energy generations in stars, nucleosynthesis, stellar explosions, and neutron stars, etc. are all affected by nuclear properties. The distinction between research in nuclear physics and nuclear astrophysics is often only in the specific application of the results [1].

## 2. Nucleosynthesis

Nucleosynthesis refers to the production of elements that constitute the baryonic matter of the universe. Operating by nuclear processes, both in the early universe and in stars, are responsible for the synthesis of the elements. This universal nuclear history of the matter is written in the compositions of its diverse constituents: stars, interstellar (and intergalactic) gas and dust, meteorites, and cosmic rays [1]. On Figure II-2, we resume the creation of elements (nucleosynthesis) on a chart.

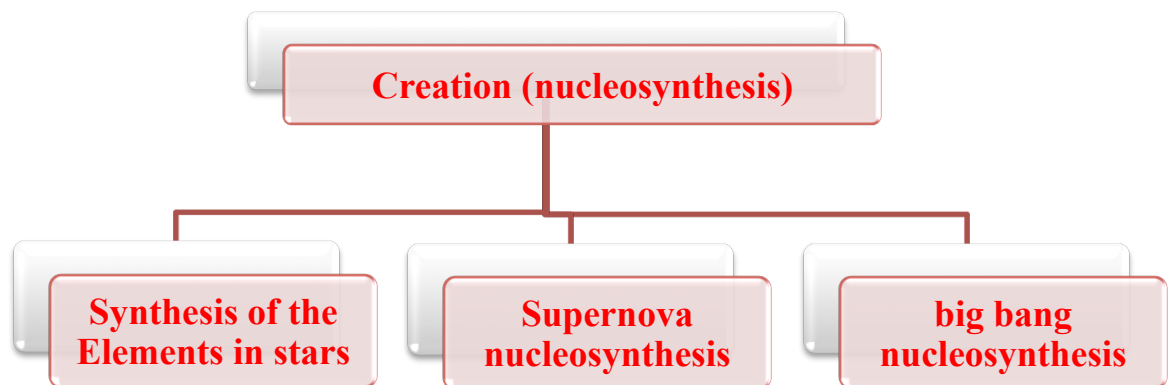


**Figure I-2:** *Chart resumes nucleosynthesis.*

### 2.1. Nucleosynthesis in the Big Bang

Nucleosynthesis in the big bang involves sequences of nuclear reactions among all the light nuclei. More accurate cross sections are needed for a number of these reactions to improve the accuracy of predicted element production in the big bang. For example deuterium synthesis the required cross sections are (in order of importance):  $d(d,n)^3\text{He}$ ,  $d(p,\gamma)^3\text{He}$ ,  $d(d,p)^3\text{H}$  and  $p(n,\gamma)d$  [1]. The history of the Big Bang is shown on Figure I-3.

In 1922, Alexander Friedmann proposed on theoretical grounds that the universe is expanding

In 1927, Lemaître also proposed what became known as the "Big Bang theory" of the creation of the universe

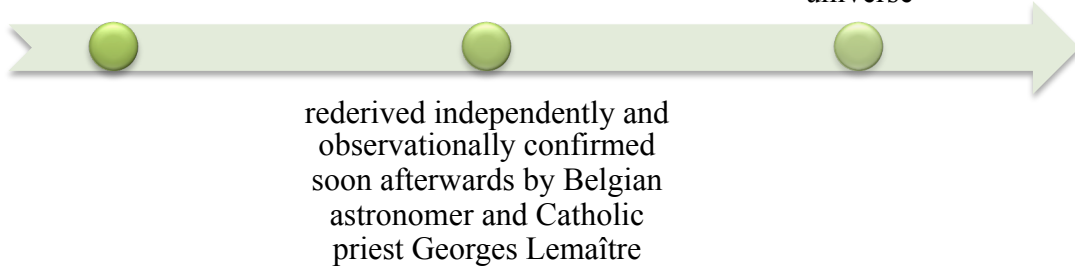


**Figure I-3:** Chart shows the “Big Bang story”.

## **2.2. Synthesis of the Elements in Stars**

A star possesses a self-governing mechanism in which the temperature is adjusted so that the outflow of energy through the star is balanced by nuclear energy generation. The temperature required to give this adjustment depends on the particular nuclear fuel available. Hydrogen requires a lower temperature than helium; helium requires a lower temperature than carbon, and so on, the increasing temperature sequence ending at iron since energy generation by fusion processes ends here [3].

Material ejected from one star may subsequently become condensed in another star. This again produces special nuclear effects [3].

### **3. Modes of Element Synthesis**

Almost all nuclei heavier than iron are made by neutron capture on lighter seed nuclei in the s- and r- processes [1]. We present on Figure I-4 some of the physical processes involved in stellar synthesis (modes), explained also in the text, that create the different elements in space.

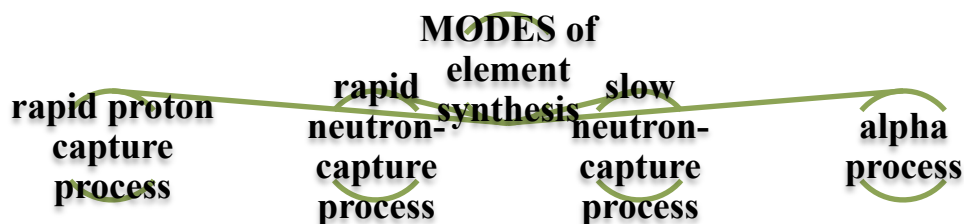


**Figure I-4:** Chart resumes modes of element synthesis.

### 3.1. The Rapid Neutron-Capture Process

Rapid neutron-capture process or so-called *r*-process, with the emission of gamma radiation ( $n,\gamma$ ), is a set of nuclear reactions that are responsible for the creation (nucleosynthesis) of approximately half the abundances of the atomic nuclei heavier than iron, usually synthesizing the entire abundance of the two most neutron-rich stable isotopes of each heavy element. Figure I-5 illustrates those nuclei produced through this process. The neutron captures occur at a rapid ( $r$ ) rate compared to the beta decays. This mode of synthesis is responsible for production of a large number of isotopes in the range  $70 \leq A \leq 209$ , and also for synthesis of uranium and thorium [3].

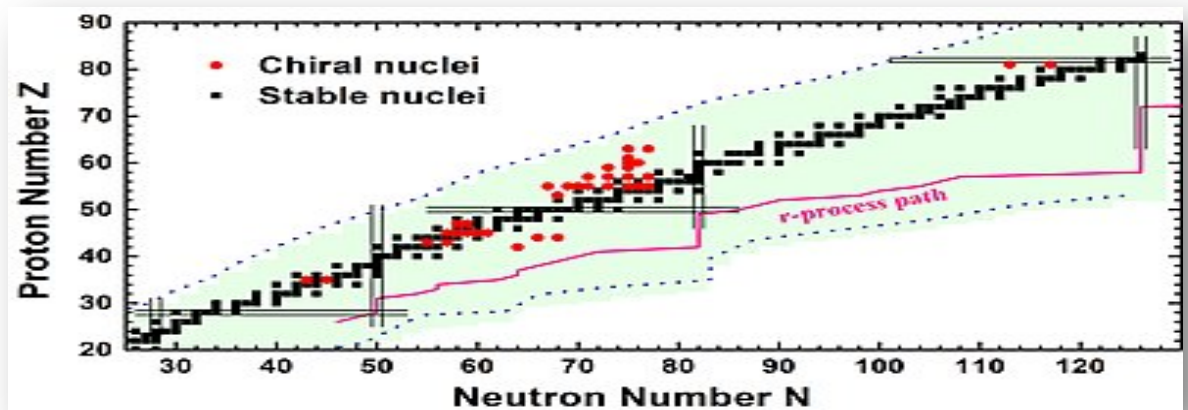


**Figure I-5:** Nuclear chart [4], on which are shown nuclei produced through the *r*-process mode.

This process may also be responsible for some light element synthesis, e.g.,  $^{36}\text{S}$ ,  $^{46}\text{Ca}$ ,  $^{48}\text{Ca}$ , and perhaps  $^{47}\text{Ti}$ ,  $^{49}\text{Ti}$ , and  $^{50}\text{Ti}$ . This produces the abundance peaks at  $A = 80$ ,  $130$ , and  $194$  [3]. The *r*-process synthesizes the other half of the nuclei heavier than iron by rapid capture of many neutrons by seed nuclei in an event lasting several seconds [1]. This mode occurs in certain conditions, we quote here the two most important ones:

- The captures must be rapid in the sense that the nuclei must not have time to undergo radioactive decay before another neutron arrives to be captured, a sequence that is halted only when the increasingly neutron-rich nuclei cannot physically retain another neutron.

- The *r*-process therefore must occur in locations where there exists a high density of free neutrons.

### 3.2. The Slow Neutron-Capture Process

Slow neutron-capture process or **s-process** is a series of reactions in nuclear astrophysics that occur in stars, particularly, in the *Asymptotic Giant Branch* (AGB) stars. The *s*-process is responsible for the creation of approximately half the atomic nuclei heavier than iron [1].

### 3.3. The Proton-Capture Process

This is the process of proton capture, called also **p-process**, with the emission of gamma radiation ( $p,\gamma$ ), or the emission of a neutron following gamma-ray absorption ( $\gamma,n$ ), which is responsible for the synthesis of a number of proton-rich isotopes having low abundance [3].

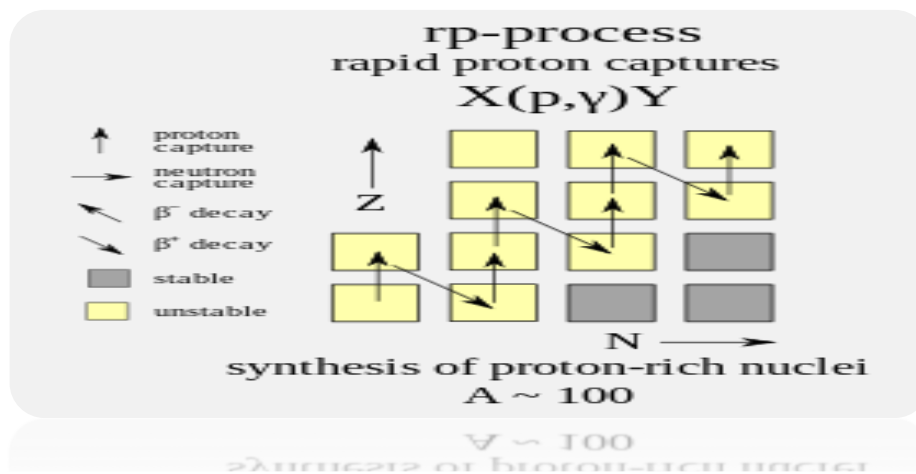


**Figure I-6:** Nucleosynthesis of proton-rich nuclei via rapid proton capture.

The rp-process is a sequence of rapid proton captures leading to the proton drip line, see Figure I-6.

#### 4. Silicon Abundance in Solar System

As the eighth most abundant element in the Universe, silicon plays an important role in understanding nucleosynthesis and *Galactic Chemical Evolution* (GCE). The main isotope  $^{28}\text{Si}$  is mainly produced by early-generation massive stars that become Type II supernovae.

The other two stable isotopes  $^{29}\text{Si}$  and  $^{30}\text{Si}$  are mainly produced by O and Ne burning in massive stars or by the s-process and by explosive burning in the final stages of stellar evolution, that is, the *Asymptotic Giant Branch* (AGB) phase for low- and intermediate-mass stars and supernova explosions for high-mass stars [5].

Stage	Time Scale	Fuel or Product	Ash or product	Temperature ( $10^9$ K)	Density ( $\text{gm}/\text{cm}^3$ )
Hydrogen	11 My	H	He	0.035	5.8
Helium	2.0 My	He	C,O	0.18	1390
Carbon	2000 y	C	Ne,Mg	0.81	$2.8 \times 10^5$
Neon	0.7 y	Ne	O,Mg	1.6	$1.2 \times 10^7$
Oxygen	2.6 y	O,Mg	Si,S,Ar, Ca	1.9	$8.8 \times 10^6$
Silicon	18 d	Si,S,Ar, Ca	Fe,Ni, Cr,Ti,...	3.3	$4.8 \times 10^7$
Iron core collapse <sup>a</sup>	~1 s	Fe,Ni, Cr, Ti,...	Neutron Star	> 7.1	$>7.3 \times 10^9$

**Table I-1:** Evolution of a 15-solar-mass star [6], My means "million years".

#### 5. Silicon-Burning Process

In astrophysics, silicon burning is a very brief sequence of nuclear fusion reactions that occur in massive stars with a minimum of about 8-11 solar masses. Silicon burning is the final stage of fusion for massive star [6]. It follows the previous stages of hydrogen, helium, carbon, neon, and Oxygen burning processes; see Table I-1 for more information about conditions and products of these burnings. When a star has completed the silicon-burning phase, no further fusion is possible. The star catastrophically Collapses and may explode in what is known as a Type II supernova [6], see Figure I-7.

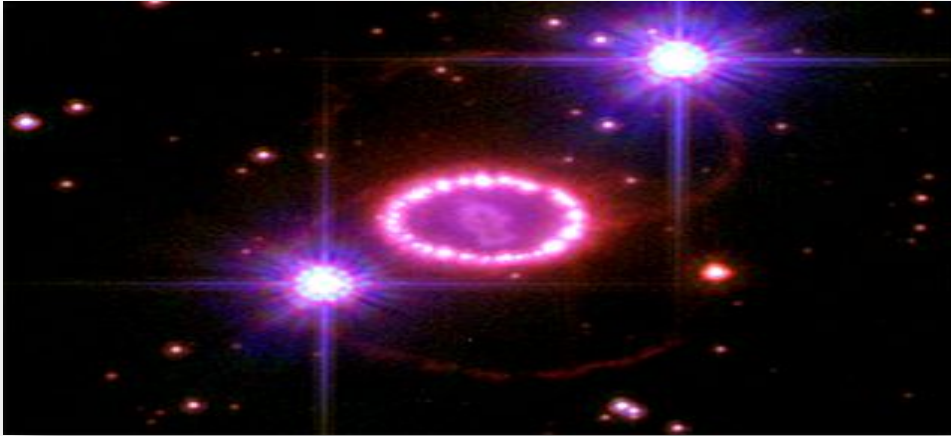
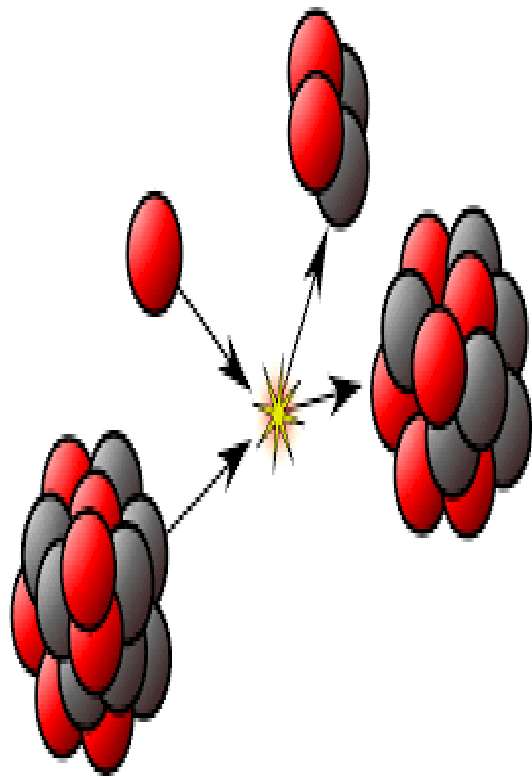
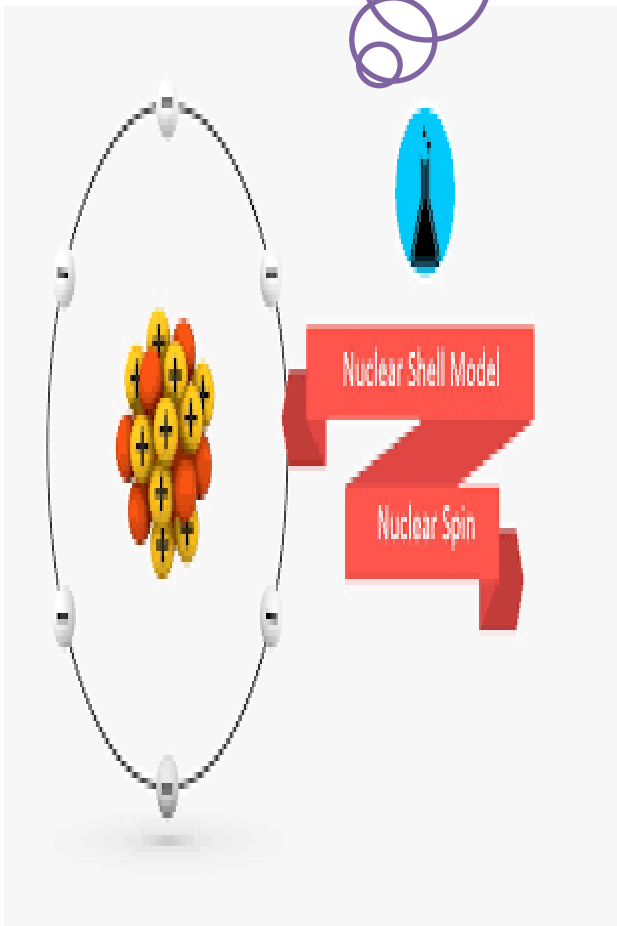


**Figure I-7:** *TYPE II-P supernova in the large Magellanic Cloud NASA image [7].*

In this chapter, we presented the astrophysical reactions occur in the stellar core and there different processes. We accentuate on the importance of Silicon in astrophysics.

In the next chapter, we will remind of the basic formalism of the nuclear shell model and the electromagnetic transitions properties. The sd shell nuclei, region of our current work, as well the PSDPF interaction, will be also introduced.

# Chapter II





# *Chapter II*

## *Shell model and sd shell nuclei*

---

Atomic nuclei are very complex systems. They are composed of many strongly interacting fermions, protons, and neutrons. The quark internal structure of the latter is important indetermination of their short-range mutual interactions, but it may not be relevant at low energies. Still, even if it is not explicitly taken into account and its effect is limited to its contribution to an interaction between nucleons, nuclear states and energies cannot be exactly calculated. As in other fields of physics, simpler models that can be solved, replace the actual systems. Successful models are sufficiently simple but still possess the important features of the system, which they represent. In spite of their complexity, nuclei exhibit some simple regularity, which are the ingredients of nuclear models. Once the neutron was discovered and it was suggested that protons and neutrons are the constituents of nuclei, it was noted that certain nuclei are more stable than others.

In this chapter, we will represent the model of the atomic nuclei, shells in nuclear structure, basic formalism of the nuclear shell model and the electromagnetic transitions properties. We, as well, introduce the sd shell nuclei properties to which we are interested.

### **1. Brief History of Nuclear Models**

#### **1.1. Liquid-Drop Model**

The earliest model of nuclear structure, based upon an analogy with a small liquid drop. This model has been developed as the droplet model, the extended droplet model, and various versions of the collective model. They have in common an emphasis on the strong local interactions of nucleons, and the implied volume and surface terms in the semi-empirical binding energy formula [8].

The liquid drop was the first model suggested to describe the nuclear structure and came before the shell model. Nevertheless, this model could not predict the binding energies of the magic nuclei that is why physics' scientists developed the shell-model, which is similar to atom's shells.

## **1.2. Shell Model**

This model is generally synonymous with the *Independent Particle Model* (IPM). The shell model places emphasis on the closure of certain IPM shells and subshells, where nuclei are found experimentally to be especially stable and/or abundant (the “magic” nuclei) [8].

Before 1945, progress in development of shell model was rather slow, because of that the model failed to reproduce binding energies of the magic nuclei. In 1949, *Mayer, Haxel Jensen* and *Suess* added the strong spin-orbit term to the single particle potential then the shell model became more acceptable [9].

## **1.3. Independent Particle Model**

The IPM is based on the Schrodinger equation that defines the energetic states of every nucleon moving under the influence of a central potential well. The states of each nucleon are uniquely determined by its five quantum numbers (n, j, ml and s).

## **2. Nuclear Shell Model and Energy Spectra**

### **2.1. Magic Numbers**

The magic number is the nucleon number at a shell closure when N or Z equals one of the numbers: 2, 8, 20, 28, 50, 82 or 126, which accorded to elements: Helium (Z=2), Oxygen (Z=8), Calcium (Z=20), Nickel (Z=28), Tin (Z=50) and Lead (Z=82). The 126 is lately added to the other precedent magic number.

### **2.2. Independent Particle**

In the independent particle model, it is assumed that the interaction between one particle and all other particles in the nucleus can be approximated by a central potential. One of the simplest choices for the central potential is the isotropic harmonic-oscillator potential, which can be written as:

$$V_{OH} = \frac{1}{2} m\omega^2 r^2 \quad (1)$$

Where m denotes the nucleon mass,  $r_i$  is the distance between nucleon and the origin of the coordinate frame.

The corresponding Hamiltonian is the sum of the single-particle’s “i” Hamiltonian as follow:

$$H_0 = \sum_i^A h_i ; h_{i0} = t_i + \frac{1}{2} m\omega^2 r^2 \quad (2)$$

So The Schrodinger equation for a nucleus in harmonic-oscillator potential has the form:

➤  $H_0\Psi = E_0\Psi$  (3)

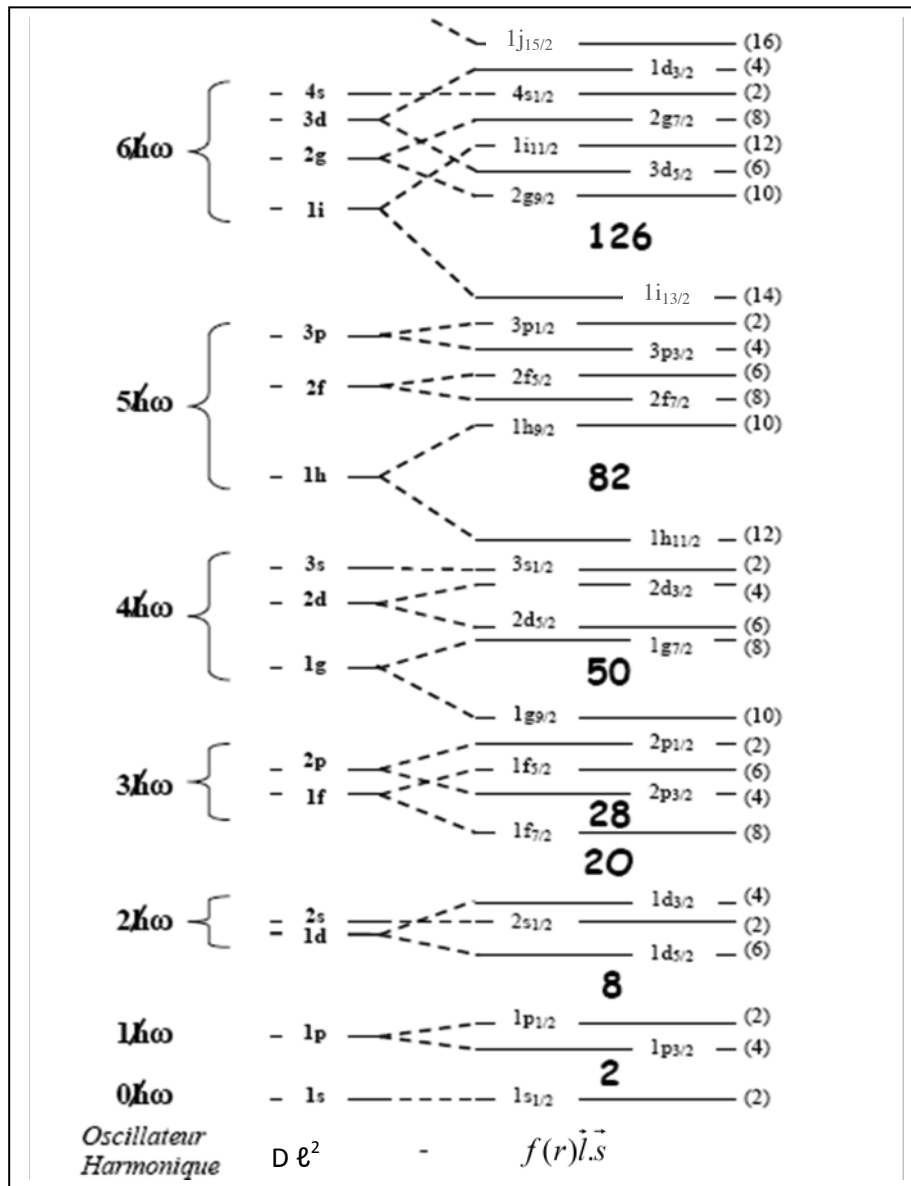


Figure II-1: Shell model single-particle orbitals.

The individual eigen-functions can be given as the product of the radial and angular coordinates

❖  $\varphi_{nlm}^i(r, \sigma) = R_{nl}(r) Y_l^{m_i}(\theta, \phi)$  (4)

❖  $E_N^i = (N + \frac{3}{2})\hbar\omega$  with  $\hbar\omega = 41A^{-1/3}$  MeV (5)

here  $\ell$  and  $m\ell$  are the quantum numbers of angular momentum and its projection, respectively, whereas  $n$  is the radial quantum number.  $N$  represents the major oscillator quantum number defined as  $N=2(n-1)+\ell$  that determine the major shells of the harmonic oscillator potential. Using the harmonic oscillator potential, we obtain only the first three

magic numbers: 2, 8, 20. A corrective term of type  $D\ell^2$  ( $D < 0$ ) has been added to the main previous Hamiltonian as [9]:

$$\text{➤ } h_{i1} = t_i + \frac{1}{2}m\omega^2 r^2 + D\ell(\ell+1)\hbar^2 \quad (6)$$

$$\text{➤ } \text{with; } E_{nl}^i = (N + \frac{3}{2})\hbar\omega + D\ell(\ell+1)\hbar^2 \quad (7)$$

Specially here, the energy degeneracy on  $\ell$  is removed but we get as well only the first three magic numbers 2, 8, 20. In the purpose to reproduce all the magic numbers, the physicists “Mayer, Jensen and Suess” introduced a strong spin-orbit coupling term to the previous Hamiltonian given by  $f(r)\vec{l}_i \cdot \vec{s}_i$ .

The total single-particle Hamiltonian becomes:

$$\text{➤ } h_i = T_i + \frac{1}{2}m\omega^2 r_i^2 + D\ell_i^2 + f(r)\vec{l}_i \cdot \vec{s}_i \quad (8)$$

The single-particle energies are given by:

$$E_{nlj}^i = (N + \frac{3}{2})\hbar\omega + D\ell(\ell+1)\hbar^2 + \frac{\hbar^2}{2} \langle f(r) \rangle_{nl} \begin{cases} -(l+1) & j = l - \frac{1}{2} \\ l & j = l + \frac{1}{2} \end{cases} \quad (9)$$

The originally degenerate single-particle levels  $j = \ell \pm \frac{1}{2}$  are split up. The radial function  $f(r)$  is negative, which means that the states with  $j = \ell + \frac{1}{2}$  are always lower in energy than the states  $j = \ell - \frac{1}{2}$ . The corresponding wave functions have the form:

$$\phi_{nljm}^i(r, \sigma) = R_{nl}(r) \sum_{m_l, m_s} \langle l m_l \frac{1}{2} m_s | j m \rangle Y_l^{m_l}(\theta, \varphi) \chi_s^{m_s}(\sigma) \quad \text{With } m = m_l + m_s \quad (10)$$

Since the nucleons are fermions, the eigen-states of a nucleus  $\Phi$  must be anti-symmetric according to the *Pauli* exclusion principle, so the wave function  $\Phi$  is a Slater determinant. The schematic representation of the single-particle energies including the three previous terms is shown on Figure II-1.

### 3. General Many Body Problem for Fermions

Consider now the case of a nucleus with  $A$  interacting nucleons ( $Z$  protons and  $N$  neutrons). We assume that these nucleons interact in pairs with the two-body interaction “ $V_{ij}$ ”. The spherical average field provides a zero-order overview of the structure of this nucleus. The correct description of such nucleus requires taking into account the 2-body interaction  $V_{ij}$ . The Hamiltonian of this nucleus becomes then [9]:

$$H = \sum_{i=1}^A (T_i + U_i) + \left( \sum_{i>j}^A v_{ij} - \sum_{i=1}^A U_i \right) = H_0 + H_r = \sum_{i=1}^A h_i + H_r \quad (11)$$

$H_0$  describes the independent movement of nucleons in a 1-body potential,

$h_i$  designates the single-particle Hamiltonian of the nucleon  $i$ ,

$\mathbf{H}_r$  represents the residual (effective) 2-body interaction that is considered to be a perturbation of the Hamiltonian  $H_0$  by a suitable choice of the average field  $\mathbf{U}$ . The determination of the latter is generally done by two methods: shell model or Hartree-Fock.

#### 4. Ingredients of the shell model

Any shell model calculation requires the implication of the following three ingredients:

- a) Definition of a valence space (inert core, active shells),
- b) derivation of an effective interaction compatible with the choice of the valence space,
- c) a code of computation to build and diagonalize the Hamiltonians.

#### Choice of the Valence Space

- The inert core: composed of closed shells (orbitals always full), usually a magic nucleus with  $Z_c$  protons and  $N_c$  neutrons.
- A valence space: contains the rest of the active nucleons ( $z = Z - Z_c$ ) and ( $n = N - N_c$ ) that interact via the  $\mathbf{H}_r$  interaction (orbitals partially occupied).
- An external space: formed of orbitals always empty.

We give here some examples of valence (model) spaces:

- ✚ The **p** shell is a space formed of both orbital  $0p_{3/2}$  and  $0p_{1/2}$ , in which can be described the properties of nuclei with  $2 < N, Z < 8$ , the inert core is the  ${}^4\text{He}$ .
- ✚ The **sd** shell valence space is composed of the three orbital  $0d_{5/2}$ ,  $1s_{1/2}$  and  $0d_{3/2}$ , only the positive parity states of nuclei with  $8 < N, Z < 20$  can be described, the inert core is the  ${}^{16}\text{O}$ .
- ✚ The **pf** shell is the space containing the four sub-shells  $0f_{7/2}$ ,  $1p_{3/2}$ ,  $0f_{5/2}$  and  $1p_{1/2}$  which is adequate for nuclei with  $20 < N, Z < 40$ , the inert core is the  ${}^{40}\text{Ca}$ .

For example, the shell model ingredients in order to reproduce both positive- and negative-parity states in sd nuclei are:

- ✓ Valence space: the full **p-sd-pf** space,
- ✓ Compatible interaction with this space: the **PSDPF** interaction,
- ✓ Code of calculation: the shell model code **NATHAN** [10, 11].

#### 5. Electromagnetic Moments and Transitions

A nucleus formed in a nuclear reaction is generally in various excited states. If these states are linked, their decay to the fundamental level is more often done by emission of gamma " $\gamma$ " radiation. The electromagnetic transitions properties can, in principle, be described by the nuclear models and, therefore, provide interesting information about the validity of the calculated wave functions of the states between which are the transitions.

The nucleon electromagnetic transition operator (the operator is an operator at 1 body) in a nucleus of mass  $A$ , between the initial level (excited energy  $E_i$ , angular momentum  $J_i$  and parity  $\pi_i$ ) and final level (excitation energy  $E_f$ , angular momentum  $J_f$  and parity  $\pi_f$ ), the nucleon emits a photon  $\gamma$  of energy  $E_\gamma$ , angular momentum  $L$  and parity  $\pi_\gamma$  :

$$E_\gamma = E_i - E_f$$

$$|J_f - J_i| \leq L \leq J_f + J_i$$

$$\pi_i \pi_\gamma \pi_f = +1$$



**Figure II-2:** Gamma emission in a nucleus.

The angular momentum of a transition is called multipolarity of the radiation. The character of the  $2^L$ -pole radiation is dipolar for  $L=1$ , quadrupolar for  $L=2$ , octupolar for  $L=3$ , and so on [8]. The multipole is of electric type **EL** when  $\pi_\gamma=(-1)^L$  and of magnetic type **ML** when  $\pi_\gamma=(-1)^{L+1}$ . As a result,  $\gamma$  transitions that connect states of the same parity have even **EL** and odd **ML**; those that connect states of different parities have odd **EL** and even **ML**. The gamma transition  $\mathbf{j}_i = \mathbf{0} \rightarrow \mathbf{j}_f = \mathbf{0}$ , do not occur because the monopole radiation  $L=0$  does not exist, since the angular momentum of the photon equals 1.

### 5.1 Electric Operator

The electric operator of a nucleus with  $A$  nucleons,  $Z$  protons and  $N$  neutrons is given by [9]:

$$O(EL) = \sum_{k=1}^A e(k) r^L(k) Y_{LM}(r(k)) \quad (12)$$

where  $e(k)$  denotes the free electric charge of a nucleon  $k$ , i.e.  $e(k)=0$  for a neutron and  $e(k)=e$  for a proton.

### 5.2 Magnetic Operator

The magnetic operator of a nucleus with  $A$  nucleons,  $Z$  protons and  $N$  neutrons is given by [9]:

$$O(ML) = \sum_{k=1}^A \mu_N \left[ g^s(k) \vec{s}(k) + \frac{2g^l(k)}{L+1} \vec{l}(k) \right] \cdot \nabla(k) r^L(k) Y_{LM}(r(k)) \quad (13)$$

where  $\mu_N = \frac{e\hbar}{2mc}$ ;  $\mu_N$  is the magnetic moment of nucleon k,  $g_l(k)$  and  $g_s(k)$  denote the orbital and spin gyromagnetic factors, respectively.

where the free orbital and spin g factors have been introduced, as [9]:

$$\begin{aligned} \color{red}{\oplus} \color{blue}{\oplus} g_s(k) &= 5.586 && \text{for a proton} \\ \color{red}{\oplus} \color{blue}{\oplus} g_s(k) &= -3.826 && \text{for a neutron} \\ \color{red}{\oplus} \color{blue}{\oplus} g_l(k) &= 1 && \text{for a proton} \\ \color{red}{\oplus} \color{blue}{\oplus} g_l(k) &= 0 && \text{for a neutron} \end{aligned}$$

### 5.3 Reduced Probabilities of Electromagnetic Transitions

The expressions of the reduced transition probabilities are given by [9]:

$$B(EL) = \frac{9}{4\pi(L+3)^2} e^2 R^{2L} \frac{\Gamma_\gamma}{\Gamma_W} \quad (e^2 fm^{2L}) \quad (14)$$

$$B(ML) = \frac{90}{\pi(L+3)^2} \mu_N^2 R^{2L-2} \frac{\Gamma_\gamma}{\Gamma_W} \quad (e^2 fm^{2L-2}) \quad (15)$$

where  $R=1.2A^{1/3}$  (fm) and e is the electric charge,  $\Gamma_\gamma$  and  $\Gamma_W$  are the transition width and the Weisskopf estimate (in eV) respectively.

$$\begin{aligned} \color{red}{\triangleright} \Gamma_W(E_1) &= 6.748 \cdot 10^{-2} A^{\frac{2}{3}} E_\gamma^3 \\ \color{red}{\triangleright} \Gamma_W(E_2) &= 4.792 \cdot 10^{-8} A^{\frac{4}{3}} E_\gamma^5 \\ \color{red}{\triangleright} \Gamma_W(E_3) &= 2.233 \cdot 10^{-14} A^2 E_\gamma^7 \end{aligned} \quad (16)$$

The strength of a transition in Weisskopf unit (W.u) is defined by the formula:  $S = \frac{\Gamma_\gamma}{\Gamma_W}$

**Notes:**

- ✓ If the initial state decreases to several final states, the total width of the initial state  $\Gamma_T$  is the sum of the partial widths:  $\Gamma_T = \sum_K \Gamma_{\gamma K}$ , therefore:  $\tau_{1/2} = \sum_K \frac{1}{\tau_{1/2}^K}$ .
- ✓ The half-life is given according to the mean lifetime:  $\tau_{1/2} = \tau_m \cdot \ln 2$ .
- ✓ We define the branching ratio (in %) of a transition k by the formula:  $BR_K = \frac{\Gamma_{\gamma K}}{\Gamma_T} \times 100$ , with  $\sum BR_K = 100$ .
- ✓ The uncertainty relation of Heisenberg:  $\Delta E \Delta t \approx \hbar$ , allows to define the width of a level (width of the gamma transition for a linked state) by:  $\Gamma = \frac{\hbar}{\tau_m}$ ,  $\hbar = 6.582 \cdot 10^{-16}$  eV.s.

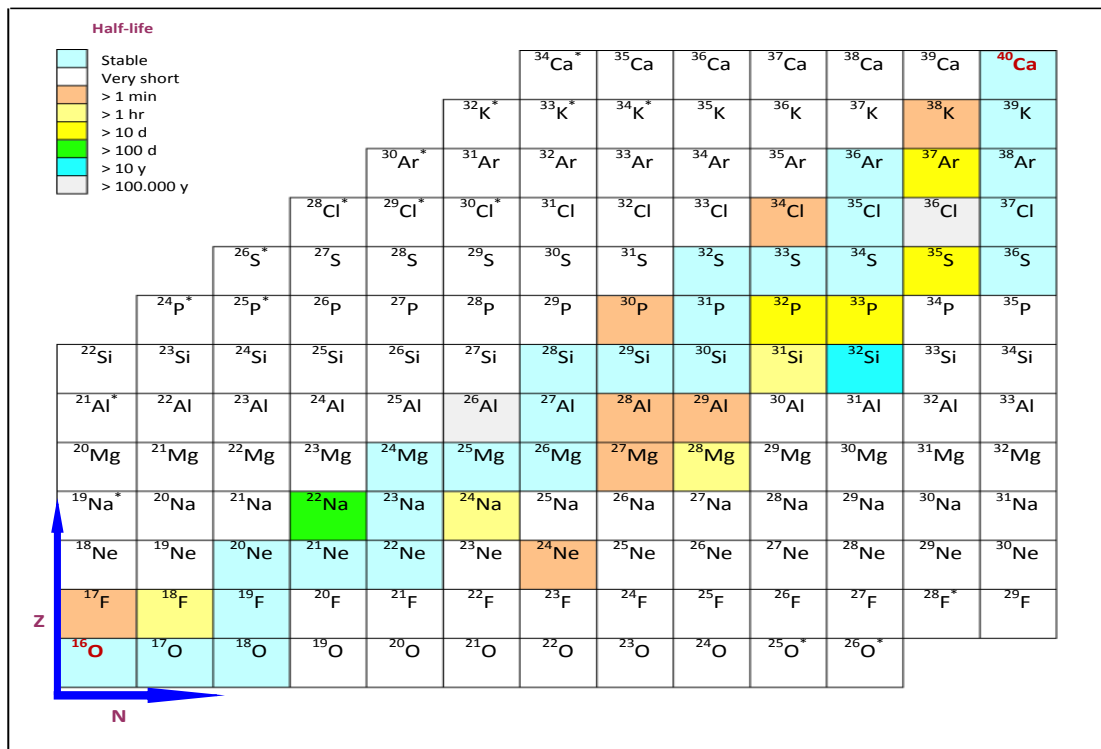


## 6 Nuclei of the sd Shell

The region of sd nuclei are those with a number of protons and neutrons comprises between 8 and 20. This area includes 146 known experimentally nuclei of which 26 are stable (Figure II-3). This region is bordered by the doubly magic nuclei  $^{16}\text{O}$  and  $^{40}\text{Ca}$ .

The experimental low excitation energy spectra [4] of these nuclei are characterized by the presence of 'normal' positive parity states (called also  $0h\omega$ ) and 'intruder' negative parity states (called  $1h\omega$ ), which are spherical. Under the shell model, the so-called normal states in which the most important orbital  $0s_{1/2}$ ,  $0p_{3/2}$ ,  $0p_{1/2}$  are occupied and the pf orbitals are empty, they have a main configuration  $(sd)^n$ , n being the number of nucleons in the sd shell. The intruder states correspond to the excitations of nucleons from the p to sd shells or sd to pf shells.

Both positive and negative parity states can simultaneously be described within the full p-sd-pf valence space and using the PSDPF interaction [12, 13], the inert core is  $^4\text{He}$ .



**FigureII-3:** *The sd shell nuclei Chart [4].*

We illustrate on Figure II-4 the distribution of protons and neutrons that formed the  $^{26}\text{Si}$  in its ground state, a nucleus of sd shell model space:

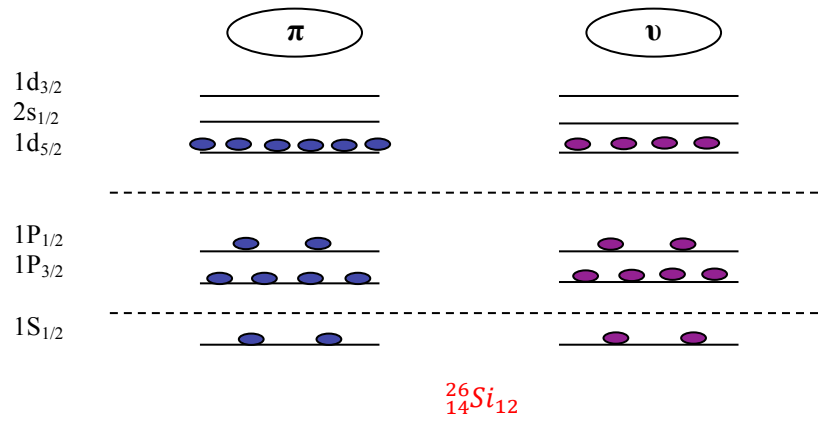


**Figure II-4:** Distribution of nucleons forming the ground state of  $^{26}\text{Si}$ .

## 7 Electromagnetic Transitions in the sd Nuclei

The PSDPF interaction has a great success in describing the 0 and 1  $\hbar\omega$  states in nuclei throughout the sd shell. This interaction has been used to calculate the energy spectra of many sd nuclei and some isotopic chains. The electromagnetic transitions, which are useful for testing the wave functions issued from the interaction, have also been investigated using the PSDPF interaction.

Electromagnetic transition observables need certain parameters, effective charges for electric transitions EL and gyromagnetic factors for magnetic ones ML. The parameters of the transitions between states of the same parities, E2 and M1, were adjusted [14] in the case of the + states using the USD or USDA/B interactions [15]. Transitions connecting opposite parity states, E1, M2 and E3, can be studied using the (0+1) $\hbar\omega$  PSDPF interaction.

**M. Labidi** studied the E3 transitions by adjusting its effective charges [16, 17]. These adjusted parameters for the three transitions E2, M1 and E3 are presented in Table II-1. Any calculation of the electromagnetic transitions in this thesis uses these parameters. For the E1 transitions, the used effective charges are:  $e_p = \frac{N}{A}e$  and  $e_n = \frac{-Z}{A}e$ .

<i>W. A. Richter et B. A. Brown [14]</i>	<i>M. Labidi [16,17]</i>	
<i>Effective charges (E2)</i>	<i>Gyromagnetic factor (M1)</i>	<i>Effective charges (E3)</i>
$e_p = 1.36$	$g_{lp} = 1.159$	$e_p = 1.36$
	$g_{sp} = 5.150$	
$e_n = 0.45$	$g_{ln} = -0.090$	$e_n = 0.48$
	$g_{sn} = -3.550$	

**Table II-2:** Adjusted parameters for E2, M1 and E3 transitions (see text).

## 8. Isospin

W. Heisenberg has conceived the isospin notion in 1932 [18]. It aims to construct a mathematical basis that represents the proton-neutron similarity with respect to the strong nuclear force. Thus, like spin multiplets of a quantum state, one combines corresponding states of nuclear isobars in an isospin multiplet. For example, the  $J^\pi = 0^+$  ground state of the mirrors  $^{26}\text{Mg}$ ,  $^{26}\text{Si}$  and the  $J^\pi = 0^+$  first excited state of  $^{26}\text{Al}$  are members of an isospin triplet. Obviously, one must remember that isospin is a useful *approximation* that neglects proton-neutron differences that are related to their mass and their electromagnetic interactions [18]. Nuclei, which are members of an isospin multiplet, have the same properties, with the exception of their electric charge, i.e. they have the same spin and almost the same mass, and members of an isospin multiplet will have the same values of these properties as well [9].

The proton and neutron are now considered to be a nucleon with different values of the third component of this isospin. Subsequently this third component can take two possible values, we assign  $t_z = -\frac{1}{2}$  for the proton and  $t_z = +\frac{1}{2}$  for the neutron. The electromagnetic interactions couple to the electric charge,  $Q$ , of the particles and in the case of nucleons this electric charge is related to the third component of isospin by [9]:

$$Q = \frac{1}{2}(1 - t_z)e \quad (17)$$

The total isospin is related to its z component as follow:

$$T_z = \sum_{i=1}^A t_{zi} = \sum_{i=1}^Z t_{zp} + \sum_{i=1}^N t_{zn} = \frac{-Z}{2} + \frac{N}{2} = \frac{(N-Z)}{2} \quad (18)$$

$$\text{and } t = |t_z|, \dots, \frac{A}{2} \quad (19)$$

In this chapter, we presented a brief formalism of the shell model. Some of the sd shell properties, after defining this area of nuclei, were as well described. We introduced the interactions developed to reproduce the spectroscopic properties and the structure of these nuclei.

In the last chapter, we will present a detailed discussion of the comparison of our results, using PSDPF, to the available experimental data for  $^{26}\text{Si}$  focusing on levels having an astrophysical interest.

# Chapter III



# ***Chapter III***

## ***Spectroscopic study of the $^{26}\text{Si}$ : levels of astrophysical interest***

---

The rapid proton capture (rp-process) is a sequence of proton capture reactions and  $\beta^+$  decays passing through proton-rich nuclei. The rp-process reaction rates are crucial nuclear physics input to astrophysical models of nucleosynthesis in novae, supernovae, and explosive hydrogen burning conditions. Silicon is one of the elements produced in space through the rp-process. We are interested to the study of the astrophysical rp reaction  $^{25}\text{Al}(p,\gamma)^{26}\text{Si}$  using the PSDPF interaction.

A detailed discussion of the current study will be presented for the  $^{26}\text{Si}$  nucleus in this chapter.

### ***1. Study of the $^{26}\text{Si}$ Spectroscopic Properties***

$^{26}\text{Si}$  is an sd shell nucleus, a set of nuclei, which start from  $^{16}\text{O}$  to  $^{40}\text{Ca}$ . Using the PSDPF interaction and the code NATHAN, we performed a shell model calculation of the excitation energy spectrum and the electromagnetic properties of  $^{26}\text{Si}$ . Since this nuclide of interest is proton-rich with  $N < Z$ , its spectrum is not well known. We used the shell-model and analog assignments of the  $T=1$  states in  $^{26}\text{Mg}$  and  $^{26}\text{Al}$  to determine the spin/parity assignments in  $^{26}\text{Si}$ , especially, those of astrophysical interest above of the proton threshold, 5513.8 keV. These levels are crucial to calculate the  $^{25}\text{Al}(p,\gamma)^{26}\text{Si}$  reaction rate.

We separated our study into two main parts, excitation energies to define all the  $J^\pi$  assignments based on shell model calculation and on the comparison to the  $T=1$  isobaric mass doublet states in  $^{26}\text{Mg}$  and  $^{26}\text{Al}$ . The second part is dedicated to the study of the known electromagnetic transitions in  $^{26}\text{Si}$ . We discuss each part separately.

#### ***1.1. Energy Spectra***

As  $^{26}_{14}\text{Si}_{12}$  has  $N < Z$ , so its spectrum is less known. We used the analog  $T=1$  states in  $^{26}\text{Mg}$  and  $^{26}\text{Al}$  to determine the  $J^\pi$  assignments in the neutron deficient nucleus  $^{26}\text{Si}$ . We discuss the  $J^\pi_i$  certainties, uncertainties, and states without  $J^\pi_i$  for the various energy regions.

<i>E(Mg)</i>		<i>E(Al)</i>			<i>E(SI)</i>		<i>Shell model</i>	
<i>E<sub>ex</sub>(Mev)</i>	<i>J<sup>π</sup></i>	<i>E<sub>ex</sub>(Mev)</i>	<i>J<sup>π</sup></i>	<i>T</i>	<i>E<sub>ex</sub>(Mev)</i>	<i>J<sup>π</sup></i>	<i>E<sub>ex</sub>(Mev)</i>	<i>J<sup>π</sup><sub>i</sub></i>
0	0 <sup>+</sup>	0	0 <sup>+</sup>	1	0	0 <sup>+</sup>	0	0 <sup>+</sup> <sub>1</sub>
1,809	2 <sup>+</sup>	1,841	(2 <sup>+</sup> )	1	1,797	2 <sup>+</sup>	1,87843	2 <sup>+</sup> <sub>1</sub>
2,938	2 <sup>+</sup>	2,932	2 <sup>+</sup>	1	2,787	2 <sup>+</sup>	3,04183	2 <sup>+</sup> <sub>2</sub>
3,589	0 <sup>+</sup>	3,525	0 <sup>+</sup>	1	3,336	0 <sup>+</sup>	3,82855	0 <sup>+</sup> <sub>2</sub>
3,942	3 <sup>+</sup>	3,964	(3 <sup>+</sup> )	1	3,758	(3 <sup>+</sup> )	3,99025	3 <sup>+</sup> <sub>1</sub>
					3,842	(4 <sup>+</sup> )		
4,333	2 <sup>+</sup>	4,32	2 <sup>+</sup>	1	4,139	2 <sup>+</sup>	4,59027	2 <sup>+</sup> <sub>3</sub>
4,35	3 <sup>+</sup>	4,371	(3 <sup>+</sup> )	1	4,187	(3 <sup>+</sup> )	4,38925	3 <sup>+</sup> <sub>2</sub>
4,319	4 <sup>+</sup>	4,477	(4 <sup>+</sup> )	1	4,446	(4 <sup>+</sup> )	4,39701	4 <sup>+</sup> <sub>1</sub>
4,901	4 <sup>+</sup>	4,904	(4 <sup>+</sup> )	1	4,797	(4 <sup>+</sup> )	5,01278	4 <sup>+</sup> <sub>2</sub>
4,835	2 <sup>+</sup>	4,913	(2 <sup>+</sup> )	1	4,811	(2 <sup>+</sup> )	4,94449	2 <sup>+</sup> <sub>4</sub>
4,972	0 <sup>+</sup>	4,967	(0 <sup>+</sup> )	1	4,831	(0 <sup>+</sup> )	4,90916	0 <sup>+</sup> <sub>3</sub>
5,292	2 <sup>+</sup>	5,316	(2 <sup>+</sup> )	1	5,148	2 <sup>+</sup>	5,50031	2 <sup>+</sup> <sub>5</sub>
					5,229	(2 <sup>+</sup> )		
5,476	4 <sup>+</sup>	5,498	(4 <sup>+</sup> )	1	5,289	4 <sup>+</sup>	5,55323	4 <sup>+</sup> <sub>3</sub>
5,716	4 <sup>+</sup>	5,696	(4 <sup>+</sup> )	1	5,518	(4 <sup>+</sup> )	5,9249	4 <sup>+</sup> <sub>4</sub>
5,691	1 <sup>+</sup>	5,8	(1 <sup>+</sup> )	1	5,676	1 <sup>+</sup>	5,69343	1 <sup>+</sup> <sub>1</sub>
					5,890	0 <sup>+</sup>		
6,125	3 <sup>+</sup>	6,136	(3 <sup>+</sup> )	1	5,929	3 <sup>+</sup>	6,2829	3 <sup>+</sup> <sub>3</sub>
6,256	0 <sup>+</sup>	6,186	(0 to 2 <sup>+</sup> )	1	5,946	0 <sup>+</sup>	6,27795	0 <sup>+</sup> <sub>4</sub>
6,634		6,573	1 <sup>+</sup> , (1 <sup>-</sup> , 2 <sup>-</sup> )	0,1	6,461	0 <sup>+</sup>	6,66761	1 <sup>+</sup> <sub>2</sub>
6,745	2 <sup>+</sup>	6,623	(2 <sup>+</sup> )	0,1	6,295	2 <sup>+</sup>	6,66772	2 <sup>+</sup> <sub>6</sub>
		6,647	(2 <sup>+</sup> )	1				
6,623	4 <sup>+</sup>	6,59	(4 <sup>+</sup> )	1		4 <sup>+</sup>	6,8154	4 <sup>+</sup> <sub>5</sub>
6,876	3 <sup>-</sup>	6,736	(3 <sup>-</sup> )	1	6,81	3 <sup>-</sup>	6,71589	3 <sup>-</sup> <sub>1</sub>
7,062	1 <sup>-</sup>	6,858	1 <sup>-</sup>	1	6,383	1 <sup>-</sup>	6,66256	1 <sup>-</sup> <sub>1</sub>
		6,913	(2 <sup>-</sup> )	(0,1)	7,154	2 <sup>-</sup>	6,73566	2 <sup>-</sup> <sub>1</sub>
6,978	5 <sup>+</sup>	6,994	(5 <sup>+</sup> )	1	7,198	5 <sup>+</sup>	7,08649	5 <sup>+</sup> <sub>1</sub>
7,542	2 <sup>-</sup>	7,025	(2 <sup>-</sup> )	1	7,496	2 <sup>-</sup>	7,69725	2 <sup>-</sup> <sub>2</sub>
7,1	2 <sup>+</sup>	7,08	(2 <sup>+</sup> )	1	7,018	2 <sup>+</sup>	6,93602	2 <sup>+</sup> <sub>7</sub>
7,283	4 <sup>-</sup>	7,12	(4 <sup>-</sup> )	1	7,522	4 <sup>-</sup>	7,89774	4 <sup>-</sup> <sub>1</sub>
		7,17	(3 <sup>-</sup> )	1	7,886			
7,349	3 <sup>-</sup>	7,181	(4 <sup>-</sup> )	1	7,701	3 <sup>-</sup>	7,49536	3 <sup>-</sup> <sub>2</sub>
7,851	2 <sup>-</sup>	7,211	0,(1,2)	1	7,418	2 <sup>-</sup>	7,95136	2 <sup>-</sup> <sub>3</sub>
7,246	3 <sup>+</sup>	7,236	(3 <sup>+</sup> )	0,1	7,674	3 <sup>+</sup>	7,34062	3 <sup>+</sup> <sub>4</sub>
		7,267	(3 <sup>+</sup> )	0,1				
					7,606			
8,034	2 <sup>-</sup>	7,269	(2 <sup>-</sup> )	(0,1)	8,008	2 <sup>-</sup>	8,1601	2 <sup>-</sup> <sub>4</sub>
		7,311	(2 <sup>-</sup> )	1	7,921			

7,371	2 <sup>+</sup>	7,333	(2) <sup>+</sup>	1		2 <sup>+</sup>	7,21409	2 <sup>+</sup> <sub>8</sub>
		7,376	(2) <sup>-</sup>	(0,1)	7,962		8,81914	2 <sup>-</sup> <sub>5</sub>
7,396	5 <sup>+</sup>	7,399	(5) <sup>+</sup>	1	8,144	5 <sup>+</sup>	7,44707	5 <sup>+</sup> <sub>2</sub>
7,428	1 <sup>+</sup>	7,585	1 <sup>+</sup>	0,1	8,254	1 <sup>+</sup>	7,92968	1 <sup>+</sup> <sub>3</sub>
7,818	2 <sup>+</sup>	7,637	(2) <sup>+</sup>	(0,1)	8,282	2 <sup>+</sup>	7,57468	2 <sup>+</sup> <sub>9</sub>
8,576	1 <sup>+</sup>	7,651	1 <sup>+</sup>	0,1	8,144	(1 <sup>-</sup> ,2 <sup>+</sup> )	8,44321	1 <sup>+</sup> <sub>4</sub>
7,677	4 <sup>+</sup>	7,663	(4) <sup>+</sup>	1	6,88	4 <sup>+</sup>	7,53007	4 <sup>+</sup> <sub>6</sub>
7,53007	4 <sup>+</sup>				8,222			
7,726	3 <sup>+</sup>	7,71	(3) <sup>+</sup>	1	8,431	3 <sup>+</sup>	7,6998	3 <sup>+</sup> <sub>5</sub>
7,774	4 <sup>+</sup>	7,725	(4) <sup>+</sup>	1		4 <sup>+</sup>	7,88299	4 <sup>+</sup> <sub>7</sub>
7,84	2 <sup>+</sup>	7,754	(2) <sup>+</sup>	1	8,356	2 <sup>+</sup>	8,37889	2 <sup>+</sup> <sub>10</sub>
8,227	1 <sup>-</sup>	7,772	(1) <sup>-</sup>	1		1 <sup>-</sup>	8,07699	1 <sup>-</sup> <sub>4</sub>
7,95	5 <sup>-</sup>	7,783	(5) <sup>-</sup>	1	8,269		8,31756	5 <sup>-</sup> <sub>1</sub>
8,052	2 <sup>+</sup>	7,836	(2) <sup>+</sup>	1	8,689	2 <sup>+</sup>	8,99252	2 <sup>+</sup> <sub>11</sub>
		7,839	(5) <sup>-</sup>	1				
		8,303	(4)	1				
8,201	6 <sup>+</sup>	8,519	(6) <sup>+</sup>	(0,1)			8,2523	6 <sup>+</sup> <sub>1</sub>
		8,696	(4)	1				
		8,832	(4)	1				
		9,043		1				
		9,058	(5)	1				
		9,083	(3 <sup>+</sup> ,4)	1				
		9,758	(7 <sup>+</sup> )	1				
7,261	1 <sup>-</sup>					1 <sup>-</sup>	7,49237	1 <sup>-</sup> <sub>2</sub>
7,697	1 <sup>-</sup>					1 <sup>-</sup>	7,7342	1 <sup>-</sup> <sub>3</sub>
7,824	3 <sup>-</sup>				8,558	3 <sup>-</sup>	7,93748	3 <sup>-</sup> <sub>3</sub>
7,2	0 <sup>+</sup>					0 <sup>+</sup>	8,06955	0 <sup>+</sup> <sub>5</sub>
8,251	3 <sup>+</sup>					3 <sup>+</sup>	8,30072	3 <sup>+</sup> <sub>6</sub>
8,399	4 <sup>-</sup>						8,39571	4 <sup>-</sup> <sub>2</sub>
8,67	5 <sup>+</sup>						8,49039	5 <sup>+</sup> <sub>3</sub>
8,706	4 <sup>+</sup>						8,68232	4 <sup>+</sup> <sub>8</sub>
8,185	3 <sup>-</sup>						8,70693	3 <sup>-</sup> <sub>4</sub>
8,93	4 <sup>+</sup>						8,75708	4 <sup>+</sup> <sub>9</sub>
8,504	1 <sup>-</sup>						8,76562	1 <sup>-</sup> <sub>5</sub>
8,625	5 <sup>-</sup>						9,06324	5 <sup>-</sup> <sub>2</sub>
8,959	1 <sup>-</sup>						9,40081	1 <sup>-</sup> <sub>6</sub>

**Table III-1:** Comparison theoretical versus experimental [4] energy spectra of the isospin mass triplet  $T=1$  states in  $A=26$  nuclei,  $^{26}\text{Mg}$ ,  $^{26}\text{Al}$ , and  $^{26}\text{Si}$ .



We have calculated, using PSDPF, the excitation energies from 0 to  $\sim 8,6$  MeV. PSDPF is a coulomb free and isospin independent interaction so it gives the same results for all the T=1 isobaric mass triplet states in A=26 nuclei,  $^{26}\text{Mg}$ ,  $^{26}\text{Al}$  and  $^{26}\text{Si}$ . The comparison of the obtained results to the experimental spectra [4] is presented in Table III-1. Note that for the  $^{26}\text{Al}$ , we subtracted the energy 228.3 keV of the first state T=1,  $0^+$  from all the T=1 states.

This spectrum contains up to 9.8 MeV totally 85 theoretical levels against 49 experimental ones in  $^{26}\text{Si}$ , 64 in  $^{26}\text{Mg}$  and 50 in  $^{26}\text{Al}$ . Among of the total states number in each nucleus from the isobaric mass triplet we have:

- 15 certain states in Si, 31 in Mg and 6 in Al. These levels have well defined  $J^\pi$ .
- 25 uncertain states in Si, 19 in Mg and 44 in Al. These states are in parenthesis with a doubt in their  $J^\pi$  assignment and have to be confirmed.
- 9 without  $J^\pi$  assignments in Si, 12 in Mg and 4 unknown parity states in  $^{26}\text{Al}$ . A prediction of their  $J^\pi$  assignments based on shell model calculation is recommended.

We remark that we have a one to one correspondence between the calculated and experimental states in all the three nuclei. The calculated levels are in good agreement with experiment, especially, in the case of Al. Some discrepancies were obtained for states colored in red that are predicted higher in energy than their experimental counterparts, which means that they have a collective character. The prediction made for many states in Si were based also on those in the Refs. [19, 20].

## **I.2. Electromagnetic Transitions**

Using the PSDPF interaction, we calculated the electromagnetic properties of states in the  $^{26}\text{Si}$  nucleus that have known half-lives. The comparison of the obtained results to the experimental data [4] is shown in Table III-2. We can see the good agreement between theory and experiment, for most states, concerning the branching ratio. All the calculated mean lifetimes have the same order of magnitude as experimental ones. This study gives more credit to the PSDPF interaction in reproducing the spectroscopic properties of nuclei even in the middle of the sd shell which could not be included in its fit.

$J_i^\pi$ $E(\text{exp})_i$ $E(\text{SM})_i$ (Mev)	$E$ $(\text{exp})_f$	$J_f^\pi$	$\tau(\text{exp})$ (S)	$\tau$ (SM) (S)	Mult (exp)	BR(exp) (%)	Mult (SM)	BR (SM) (%)
1,797 $2_1^+$ 1,87843	0,0	$0_1^+$	6,35E-13	9,13E-13	<b>E2</b>	100	<b>E2</b>	100
2,787 $2_2^+$ 3,04183	1,797 0,0	$2_1^+$ $0_1^+$	2,11E-13	1,35E-13	<b>M1+E2</b> <b>E2</b>	32,8 (18) 67,2 (18)	<b>M1+E2</b> <b>E2</b>	35,6 64,4
3,336 $0_2^+$ 3,82855	2,787 1,797	$2_2^+$ $2_1^+$	2,19E-12	3,47E-10	<b>E2</b>	< 2 98 (19)	<b>E2</b> <b>E2</b>	1,22 98,8
3,758 $3_1^+$ 3,99025	2,787 1,797	$2_2^+$ $2_1^+$	6,997E-13	1,70E-12	<b>M1+E2</b> <b>M1+E2</b>	45 (2) 55 (2)	<b>M1+E2</b> <b>M1+E2</b>	43,7 56,3
4,139 $2_3^+$ 4,59027	3,336 2,787 1,797 0,0 3,758	$0_2^+$ $2_2^+$ $2_1^+$ $0_1^+$ $3_1^+$	9,09E-14	9,09E-14	<b>M1+E2</b> <b>(E2)</b>	<9,3 3,8 (6) 77,7 (16) 9,2 (46)	<b>E2</b> <b>M1+E2</b> <b>M1+E2</b> <b>E2</b> <b>M1+E2</b>	0,26 14,8 74,7 10,3 0,01
4,188 $3_2^+$ 4,38925	2,787 1,797 4,139 3,758	$2_2^+$ $2_1^+$ $2_3^+$ $3_1^+$		7,82E-14		63,5 (37) 36,5 (37)	<b>M1+E2</b> <b>M1+E2</b> <b>M1+E2</b> <b>M1+E2</b>	27,6 72,1 0,001 0,289
4,446 $4_1^+$ 4,39701	2,787 1,797 4,139 3,758 4,188	$2_2^+$ $2_1^+$ $2_3^+$ $3_1^+$ $3_2^+$	5,049E-13	2,98E-13	<b>E2</b>	9 (5) 90,91 (20)	<b>E2</b> <b>E2</b> <b>E2</b> <b>M1+E2</b> <b>M1+E2</b>	4,24 62,76 32,3 0,58 0,006

4,797	$4_2^+$ 5,01278	1,797 2,787 4,139 3,758 4,188 4,446	$2_1^+$ $2_2^+$ $2_3^+$ $3_1^+$ $3_2^+$ $4_1^+$	5,39E-14		100	E2 E2 E2 M1+E2 M1+E2 M1+E2	94,9 2,58 0,002 0,14 2,22 0,180
4,811	$2_4^+$ 4,94449	1,797 2,787 4,139 3,758 4,188 4,446 0,0 3,336	$2_1^+$ $2_2^+$ $2_3^+$ $3_1^+$ $3_2^+$ $4_1^+$ $0_1^+$ $0_2^+$	9,95E-14	5,40E-14	91 (11)	M1+E2 M1+E2 M1+E2 M1+E2 M1+E2 E2 E2 E2	71,9 5,13E 0,059 5,86 4,47 0,001 11,5 1,09
				<10		<9		

**Table III-2:** Comparison experimental [4] versus calculated spectroscopic properties of the  $^{26}\text{Si}$ .

## 2. States of Astrophysical Interest in $^{26}\text{Si}$

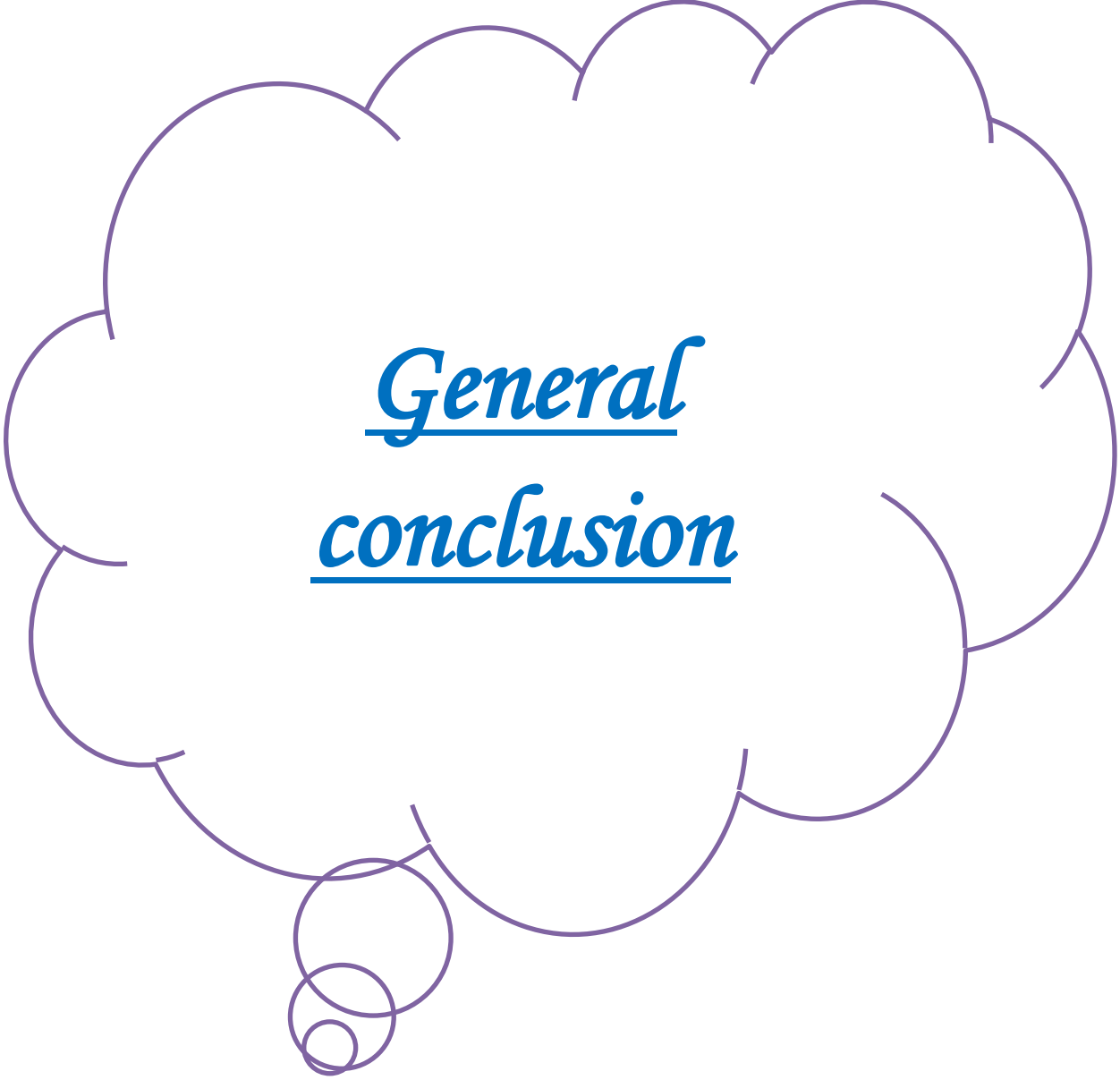
Among of silicon isotopes, the  $^{26}\text{Si}$  has a significant interest in astrophysics. The level structure of  $^{26}\text{Si}$  is also a key to understand the nucleosynthesis and energy generation, because it plays an important role in the calculation of  $^{25}\text{Al}(p,\gamma)^{26}\text{Si}$  stellar reaction rate. This reaction itself is important for understanding explosive hydrogen burning environments like novae. The  $J^\pi$  assignments for levels above the proton threshold, 5513.8 keV, are crucial for the reaction rate determination. We propose on Table III-3 the  $J^\pi$  assignments of states of astrophysical interest in  $^{26}\text{Si}$ . We think now that the reaction rate can be calculated based on this study.

<i>E(SI)</i>		<i>Shell model</i>	
$E_{ex}(\text{Mev})$	$J^{\pi}$	$E_{ex}(\text{Mev})$	$J^{\pi}_i$
<b>5,518</b>	$(4^+)$	5,9249	$4^+_4$
5,676	$1^+$	<b>5,69343</b>	$1^+_1$
5,890	$0^+$		
5,929	$3^+$	<b>6,2829</b>	$3^+_3$
5,946	$0^+$	<b>6,27795</b>	$0^+_4$
6,461	$0^+$	<b>6,66761</b>	$1^+_2$
6,295	$2^+$	<b>6,66772</b>	$2^+_6$
	$4^+$	<b>6,8154</b>	$4^+_5$
6,81	$3^-$	<b>6,71589</b>	$3^-_1$
<b>6,383</b>	$1^-$	<b>6,66256</b>	$1^-_1$
7,154	$2^-$	<b>6,73566</b>	$2^-_1$
7,198	$5^+$	<b>7,08649</b>	$5^+_1$
7,496	$2^-$	<b>7,69725</b>	$2^-_2$
7,018	$2^+$	<b>6,93602</b>	$2^+_7$
7,522	$4^-$	<b>7,89774</b>	$4^-_1$
7,886			
7,701	$3^-$	<b>7,49536</b>	$3^-_2$
7,418	$2^-$	<b>7,95136</b>	$2^-_3$
7,674	$3^+$	<b>7,34062</b>	$3^+_4$
7,606			
8,008	$2^-$	<b>8,1601</b>	$2^-_4$
7,921			
	$2^+$	<b>7,21409</b>	$2^+_8$
7,962		<b>8,81914</b>	$2^-_5$
8,144	$5^+$	<b>7,44707</b>	$5^+_2$
8,254	$1^+$	<b>7,92968</b>	$1^+_3$
8,282	$2^+$	<b>7,57468</b>	$2^+_9$
8,144	$(1^-, 2^+)$	<b>8,44321</b>	$1^+_4$
<b>6,88</b>	$4^+$	<b>7,53007</b>	$4^+_6$
8,222			
8,431	$3^+$	<b>7,6998</b>	$3^+_5$
	$4^+$	<b>7,88299</b>	$4^+_7$
8,356	$2^+$	<b>8,37889</b>	$2^+_{10}$
	$1^-$	<b>8,07699</b>	$1^-_4$
8,269		<b>8,31756</b>	$5^-_1$

8,689	$2^+$	8,99252	$2^+_{11}$
		8,2523	$6^+_1$
	$1^-$	7,49237	$1^-_2$
	$1^-$	7,7342	$1^-_3$
8,558	$3^-$	7,93748	$3^-_3$

**Table III-3:**  $J^\pi$  assignments proposed for levels in  $^{26}\text{Si}$  having astrophysical interest.

In this chapter, we studied the spectroscopic properties of the  $^{26}_{14}\text{Si}_{12}$  nucleus using the PSDPF interaction. As we have shown, the PSDPF interaction describes quit well these properties. This study led us to confirm the uncertain states (levels with uncertain  $J^\pi$ ) and to predict  $J^\pi$  assignments for the unidentified ones (states with unknown  $J^\pi$ ). The  $J^\pi$  assignments for states of astrophysical interest were also proposed.



*General*  
*conclusion*

## *General conclusion*

---

**A**mong of silicon isotopes,  $^{26}\text{Si}$  has a significant interest in astrophysics. The level structure of  $^{26}\text{Si}$  is also a key to understand the nucleosynthesis and energy generation.

The main aim of our work was the calculation of the spectroscopic properties, excitation energy spectrum, and electromagnetic transitions, using the PSDPF interaction of  $^{26}\text{Si}$ . This study is very important in order to determine the spin/parity assignments for states of astrophysical interest above of the proton threshold, 5513.8 keV. These levels are essential to calculate the  $^{25}\text{Al}(p,\gamma)^{26}\text{Si}$  reaction rate.

The obtained results show a good arrangement theory versus experiment for all the spectroscopic properties of the  $^{26}\text{Si}$ . In order to determine the  $J^\pi$  of the uncertain levels in this nucleus, we used its T=1 isobaric mass doublet,  $^{26}\text{Mg}$  and  $^{26}\text{Al}$ .

This study allowed us to confirm the undefined states and to predict spin and/ or parity assignments for the unknown states. These predictions were made using not only the comparison between calculated and experimental excitation energies for each state but also taking into account the electromagnetic transitions issued from these states or feeding them as well the reaction types in which they are observed.

The  $^{25}\text{Al}(p,\gamma)^{26}\text{Si}$  stellar reaction rate can now be calculated based on our study.

# Bibliography

---

- [1] “Opportunities in nuclear astrophysics”, Conclusions of a Town Meeting held at the University of Notre Dame, 7-8 June 1999. Prepared by the Joint Institute for Nuclear Astrophysics Michigan State University and the University of Notre Dame.
- [2] Lodders K., Palme H., Gail HP. (2009) 4.4 Abundances of the elements in the Solar System. In: Trümper J. (eds) Solar System. Landolt-Börnstein - Group VI Astronomy and Astrophysics (Numerical Data and Functional Relationships in Science and Technology), vol 4B. Springer, Berlin, Heidelberg
- [3] E. M. Burbidge, G. R. Burbidge, W. A. Fowler and F. Hoyle, *Rev. Mod. Phys.* 29, 547 (1957).
- [4] <http://www.nndc.bnl.gov/nudat2>
- [5] T. C. Peng *et al.*, *Astron & Astrophys.* 559, L8 (2013).
- [6] S. Woosley and T. Janka, *Nat. Phys.* 1, 147 (2005).
- [7] [https://en.wikipedia.org/wiki/Type\\_II\\_supernova#/media/File:HST\\_SN\\_1987A\\_20th\\_anniversary.jpg](https://en.wikipedia.org/wiki/Type_II_supernova#/media/File:HST_SN_1987A_20th_anniversary.jpg)
- [8] Norman D. Cook, “Models of the Atomic Nucleus With Interactive Software”, Springer, (2006).
- [9] P.J. Brussaard, P.W.M. Glaudemans, “Shell–Model Applications in Nuclear Spectroscopy”, North–Holland, (1977).
- [10] E. Caurier, F. Nowacki, *Acta Phys. Pol. B* 30, 705 (1999).
- [11] E. Caurier, G. Martinez-Pinedo, F. Nowacki, A. Poves, and A. P. Zuker, *Rev. Mod. Phys.* 77, 427 (2005).
- [12] M. Bouhelal, F. Haas, E. Caurier, F. Nowacki, A. Bouldjedri, *Nucl. Phys. A* 864, 113, (2011).
- [13] M. Bouhelal, Ph.D. thesis, under joint supervision of University of Batna, Batna, Algeria, and University of Strasbourg, Strasbourg, France, 2010.
- [14] W. A. Richter, S. Mkhize, and B. Alex Brown, *Phys. Rev. C* 78, 064302 (2008).



- [15] B. A. Brown, W. A. Richter, Phys. Rev. C 74, 034315 (2006).
- [16] M. Labidi, Master's thesis, University of Tebessa, Algeria (2013).
- [17] M. Bouhelal, M. Labidi, F. Haas, and E. Caurier, Phys. Rev. C 96, 044304 (2017).
- [18] E. Comay, Prog. in Phys. 4, 55 (2011).
- [19] W. A. Richter, B. A. Brown, A. Signoracci, and M. Wiescher, Phys. Rev. C 83, 065803 (2011).
- [20] C. Iliadis, L. Buchmann, P. M. Endt, H. Herndl and M. Wiescher, Phys. Rev. C 53, 475 (1996).